

International
Progress Report

IPR-01-03

Äspö Hard Rock Laboratory

Long-Term Diffusion Experiment

Microscopic observation of disturbance in drill core samples from KA3065A02 and KA3065A03

Chunlin Li

Luleå University of Technology

January 2001

Svensk Kärnbränslehantering AB

Swedish Nuclear Fuel
and Waste Management Co
Box 5864
SE-102 40 Stockholm Sweden
Tel +46 8 459 84 00
Fax +46 8 661 57 19



Äspö Hard Rock
Laboratory

Report no.	No.
IPR-01-03	F79K
Author	Date
C Li	01-01-01
Checked by	Date
Anders Winberg	01-02-01
Approved	Date
Christer Svemar	01-02-01

Äspö Hard Rock Laboratory

Long-Term Diffusion Experiment

Microscopic observation of disturbance in drill core samples from KA3065A02 and KA3065A03

Chunlin Li

Luleå University of Technology

January 2001

Keywords: Core, LTDE, micro crack, microscope, sample disturbance, scan line, thin section

This report concerns a study which was conducted for SKB. The conclusions and viewpoints presented in the report are those of the author(s) and do not necessarily coincide with those of the client.

CONTENTS	PAGE
1 INTRODUCTION	2
2 SAMPLES AND SAMPLE PREPARATION.....	3
3 METHOD FOR CRACK MAPPING.....	6
3.1 INSTRUMENT	6
3.2 SCAN LINES AND MAPPING CELLS	6
4 RESULTS AND EVALUATION	9
4.1 NUMBER OF CRACKS	9
4.2 SKETCHES OF CRACKS.....	14
5 DISCUSSION.....	17
5.1 DISTRIBUTION OF CRACKS	17
5.2 HETEROGENEITY IN CRACK DISTRIBUTION	17
5.3 CHARACTERISTICS OF CRACKS.....	18
5.4 HYPOTHESIS FOR THE MECHANISM OF THE MICROCRACKS	19
6 CONCLUSIONS.....	21
7 RECOMMENDATIONS	22
8 ACKNOWLEDGEMENT	23
9 REFERENCES	24
APPENDIX - RESULTS OF CRACK COUNT IN THIN SECTIONS	25

1 Introduction

The planned work is a part of the project "Tracer retention understanding experiments - Long-term diffusion experiment (LTDE)". The objective of LTDE is to assess the in situ diffusion characteristics of crystalline rock. The objective of the present work is to determine the distribution as well as the homogeneity of the disturbance /damage in drill core samples from two boreholes in Äspö Hard Rock Laboratory (HRL), which have been drilled as part of the LTDE project.

2 Samples and sample preparation

Totally seven thin sections were prepared from two rock cores, one with a diameter of $\phi 177$ mm and the other with a diameter of $\phi 45$ mm. The $\phi 177$ mm core was taken from borehole KA3065A03 and the $\phi 45$ mm core from borehole KA3065A02.

In preparation of the thin sections, small rock piece samples (about 1 mm thick) were cut from the cores. The side of the samples that will be glued to the glass was polished with three types of grind papers, from coarse to fine. The samples were then heated to 50 °C, exposed to vacuum and saturated with a fluorescent epoxy (Araldite D from Ciba with the fluorescent additive Epodye from Struvers) for about 3 to 5 minutes. After that, they were glued to glass plates and heated for about 3 hours. The samples glued on glasses were then polished in a machine to about 50 μm and finally by hand to about 25 μm thick for microscope observation.

Five thin section samples were prepared from the $\phi 177$ mm core and two from the $\phi 45$ mm core. All the seven thin section samples are illustrated in Table 2.1. The position and orientation of the thin sections in the corresponding cores are illustrated in Figures 2.1 and 2.2.

Thin sections A1, B1, B2 and C1 are prepared in the cross section of the cores, i.e., in plans orthogonal to the axis of the cores, while Ax, Bx and Cx are prepared in plans parallel with the axis of the cores. For the sake of simplicity, thin sections A1, B1, B2 and C1 are called “orthogonal samples”, while Ax, Bx and Cx are called “axial samples” in this report.

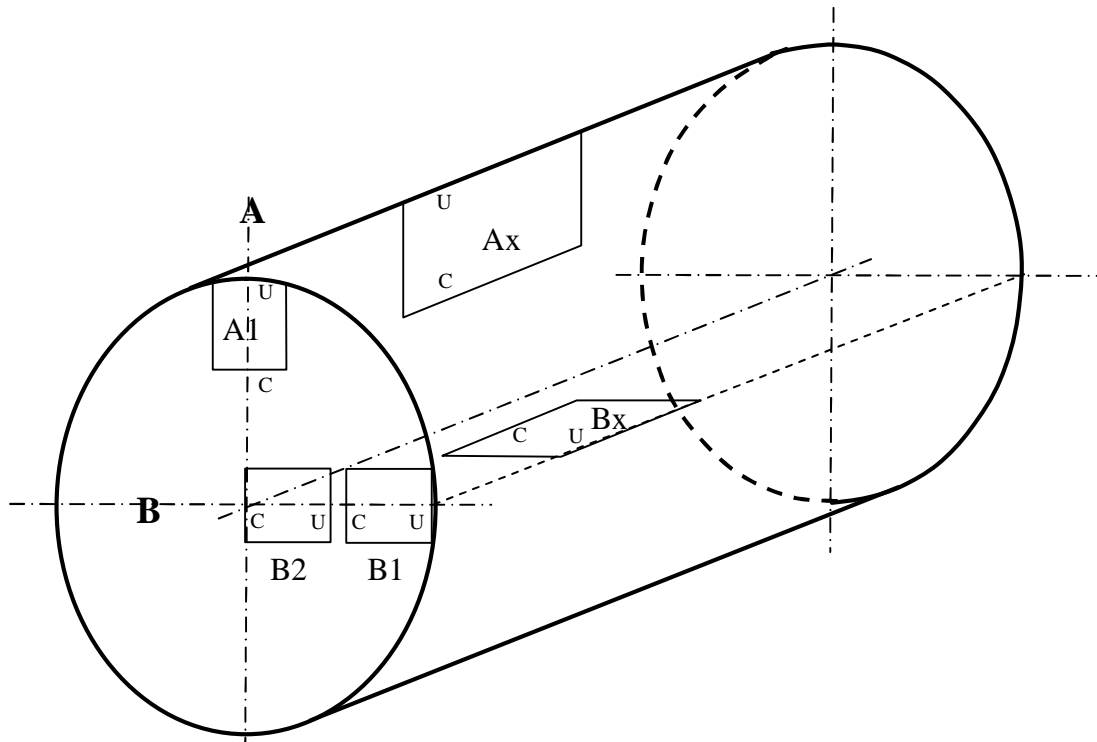


Figure 2.1 The positions of the thin sections A1, Ax, B1, B2 and Bx in the $\phi 177\text{mm}$ core.

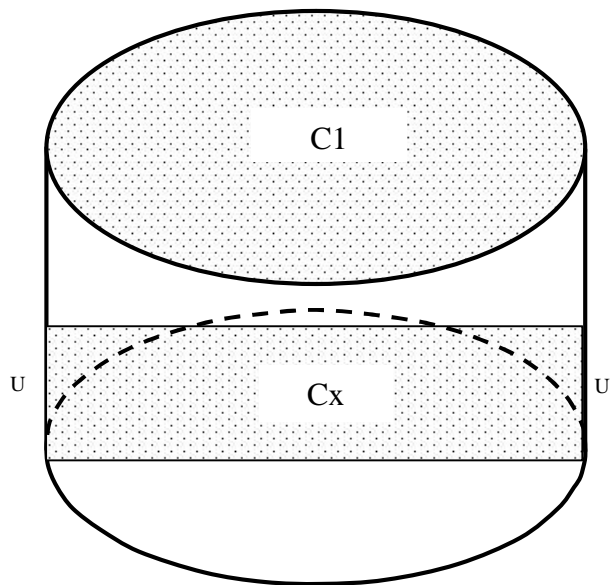
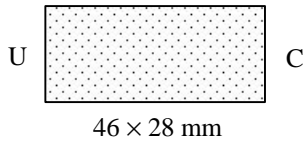

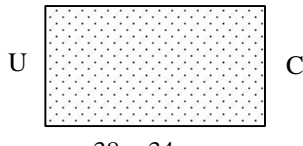

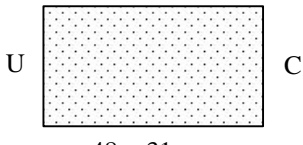
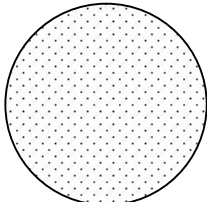
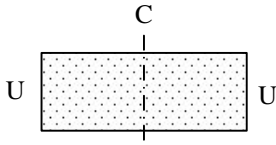


Figure 2.2 The positions of the thin sections C1 and Cx in the $\phi 45\text{ mm}$ core.

Table 2.1 Geometrical description of the thin section samples.

Thin section No.	Shape and dimension of the thin section	Borehole
A1	 <p>46 × 28 mm</p>	KA3065A03
Ax	 <p>46 × 33 mm</p>	KA3065A03
B1	 <p>38 × 34 mm</p>	KA3065A03
B2	 <p>40 × 35 mm</p>	KA3065A03
Bx	 <p>48 × 31 mm</p>	KA3065A03
C1	 <p>φ45 mm</p>	KA3065 A02
Cx	 <p>45 × 20 mm</p>	KA3065 A02

Note: Letter "C" refers to the edge towards the core centre. Letter "U" refers to the periphery of the core in all the samples except in B2. In B2 "U" refers the edge of the thin section, which faces the "C" edge of B1, see Figure 2.1.

3 Method for crack mapping

3.1 Instrument

The instrument used for crack mapping is a conventional microscope with a magnification of 50.

3.2 Scan lines and mapping cells

Five parallel scan lines, starting at the periphery of the core (the "U" edge in the thin section) and extending towards the centre of the core (the "C" edge in the thin section), are drawn in all the rectangular thin sections, see Figures 3.1, 3.2 and 3.4. Every scan line is divided into a number of consequent, non-overlapping mapping cells (3 mm wide), which are numbered by 1, 2, 3..., starting at the "U" edge. Five radial scan lines are drawn in the circular thin section C1 prepared from the $\phi 45\text{mm}$ rock core, see Figure 3.3.

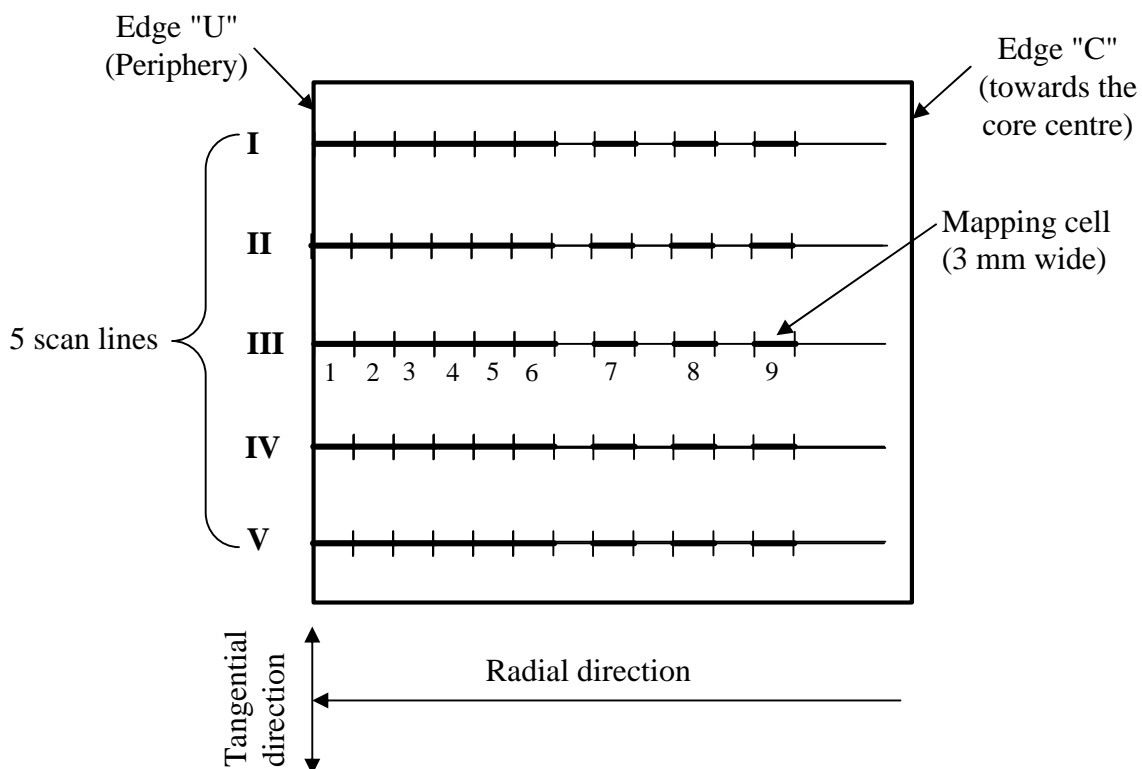


Figure 3.1 Scan lines and mapping cells in thin sections A1, Ax, B1 and Bx from borehole KA3065A03.

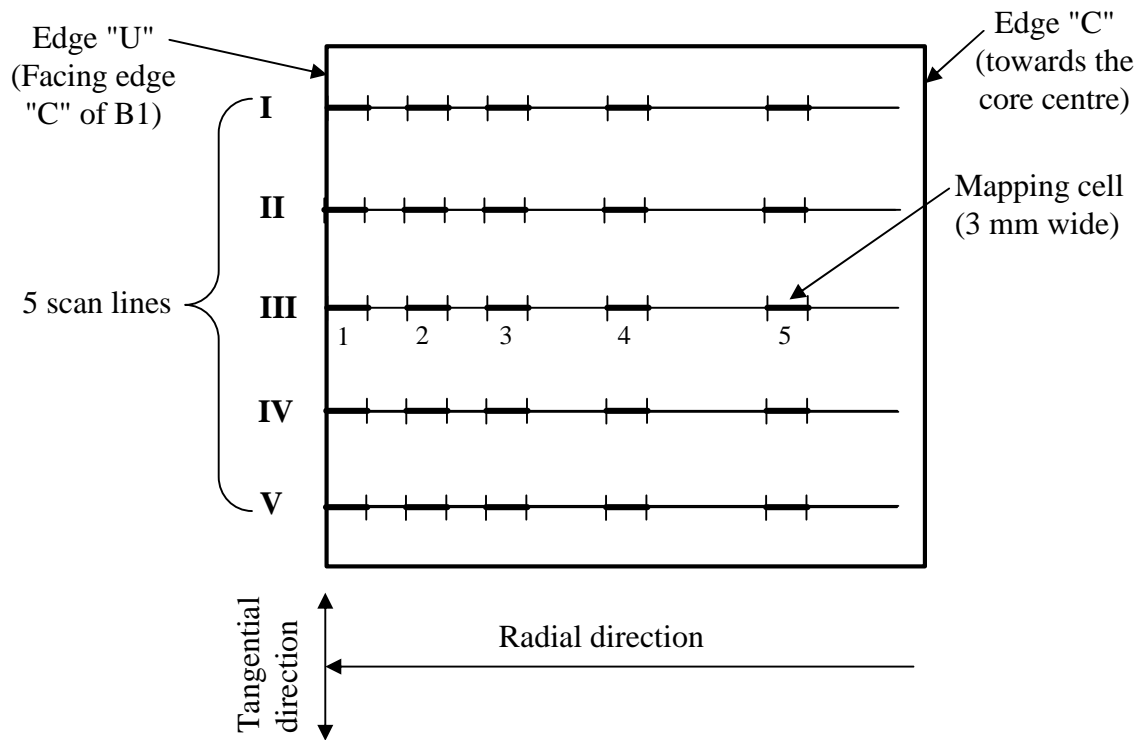


Figure 3.2 Scan lines and mapping cells in thin section B2 from KA3065A03.

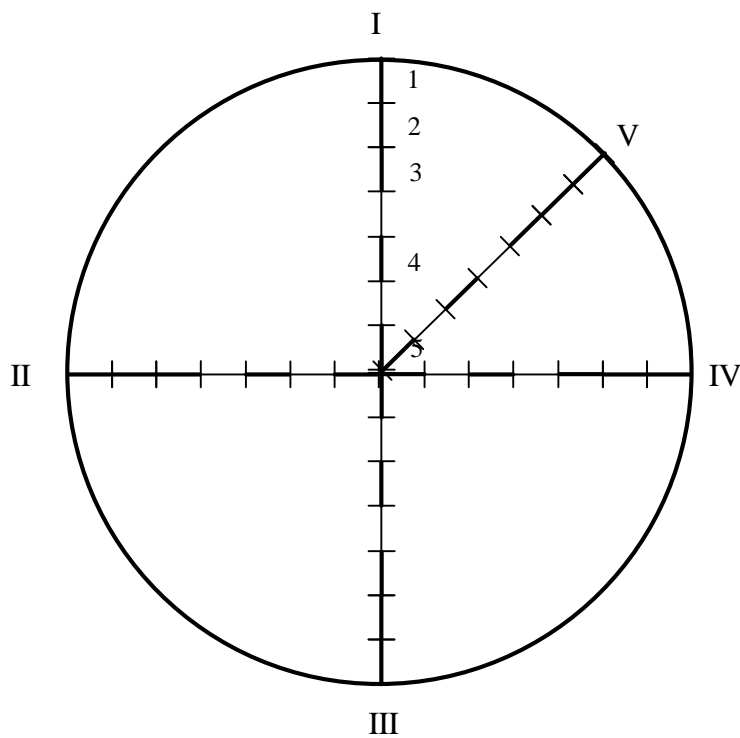


Figure 3.3 Scan lines and mapping cells in thin section C1 from borehole KA3065A02.

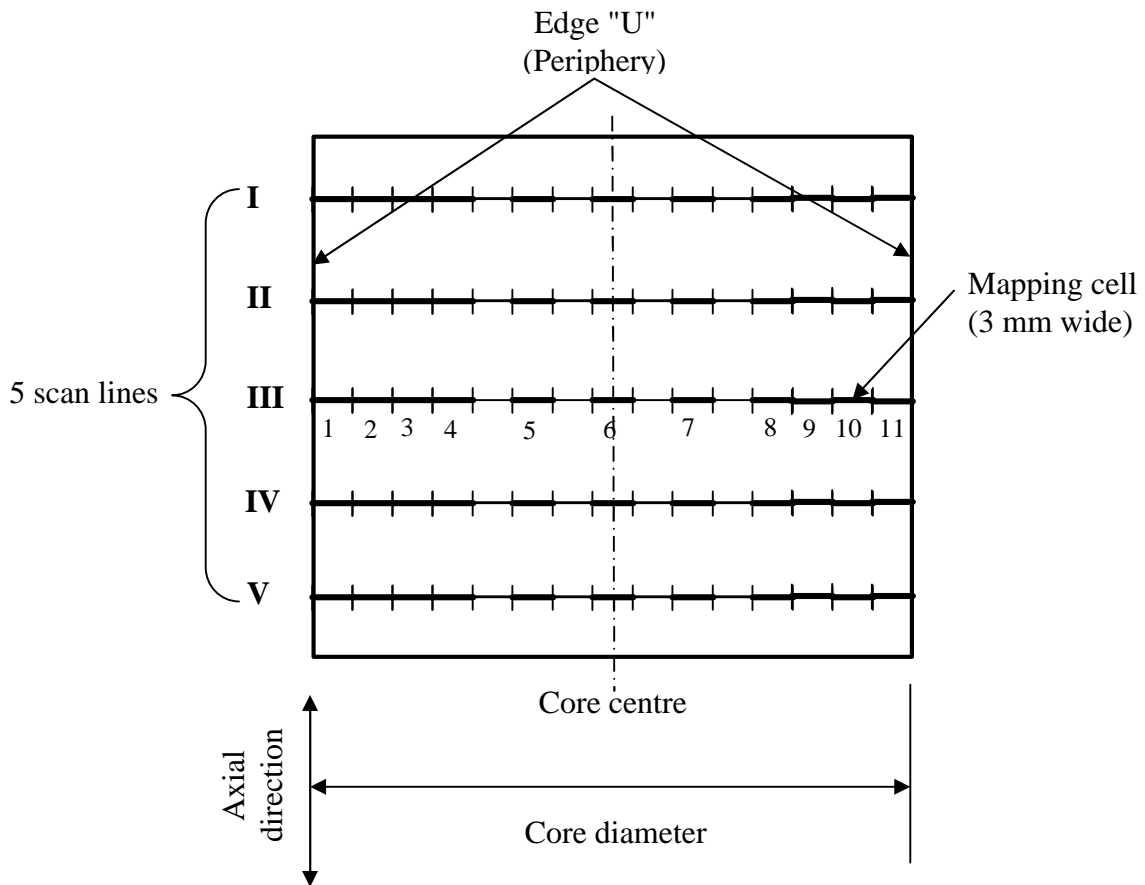


Figure 3.4 Scan lines and mapping cells in thin section Cx from borehole KA3065A02.

4 Results and Evaluation

4.1 Number of cracks

The number of cracks traversing the scan lines is counted in each mapping cell. The results of the crack counts in all the cells are summarised in the tables of Appendix. As seen in Figures 3.1-3.4, all the cells with identical numbers on the five scan lines have the same distance to the periphery. For every cell number, for instance cell 1, we have five crack counts, counted in the five cells on the scan lines I, II, III, IV and V, respectively. The mean values of the five counts mapped in each cell No. are presented in Table 4.1 for all the seven samples. The crack counts in all the cells as well as the mean values of every cell No. are presented in Figures 4.1 – 4.6. The crack counts for samples B1 and B2 are presented in the same diagram (Figure 4.2) since they were prepared in the same cross section and along the same radius. The gap between these two samples was assumed to be 3 mm in calculating the distances of the cells in sample B2.

The variation of the crack density in a sample can be expressed by the standard deviation of the crack counts. The overall standard deviation of the crack counts for every sample is defined as:

$$\text{STD dev} = \sqrt{\frac{1}{N(5-1)} \sum_{i=1}^5 \sum_{j=1}^V (X_{ij} - \bar{X}_i)^2}$$

where N stands for the largest cell No., for instance, N=9 for sample A1. X_{ij} represents the crack count mapped in the cell No. i on scan line j. \bar{X}_i represents the mean value of the crack counts in the cell No. i over all the five scan lines. The overall standard deviations of the crack counts for all the samples are listed in the bottom of Table 4.1.

Table 4-1 The mean values and standard deviations of the mapped number of cracks.

Cell No.	Distance to periphery (mm)	Samples						
		KA3965A03					KA3965A02	
		A1	B1	B2	Ax	Bx	C1	Cx
1	1.5	7.8	8.2		1.6	2.2		
2	4.5	4.4	5.2		2.0	2.0		
3	7.5	3.4	5.4		3.0	2.8		
4	10.5	4.4	5.6		1.4	2.6		
5	13.5	5.4	4.2		2.2	2.0		
6	16.5	3.2	4.0		2.0	2.4		
7	22.5	3.4	4.0		1.8	1.8		
8	28.5	3.4	3.6		2.0	3.6		
9	34.5	3.6	3.4		2.8	3.2		
1	42.5			4				
2	48.5			3				
3	54.5			3,2				
4	63.5			1				
5	75.5			1,8				
1	1.5						1.0	
2	4.5						1.4	
3	7.5						2.4	
4	13.5						2.0	
5	19.5						2.6	
	Distance to the core center (mm)							
1	-21							1.2
2	-18							2.8
3	-15							1.8
4	-12							1.2
5	-6							2.8
6	0							3.2
7	6							1.2
8	12							1.8
9	15							1.8
10	18							2.4
11	21							2.4
Overall STD deviation:		1.3	2.1	1.7	1.0	1.3	0.9	1.3

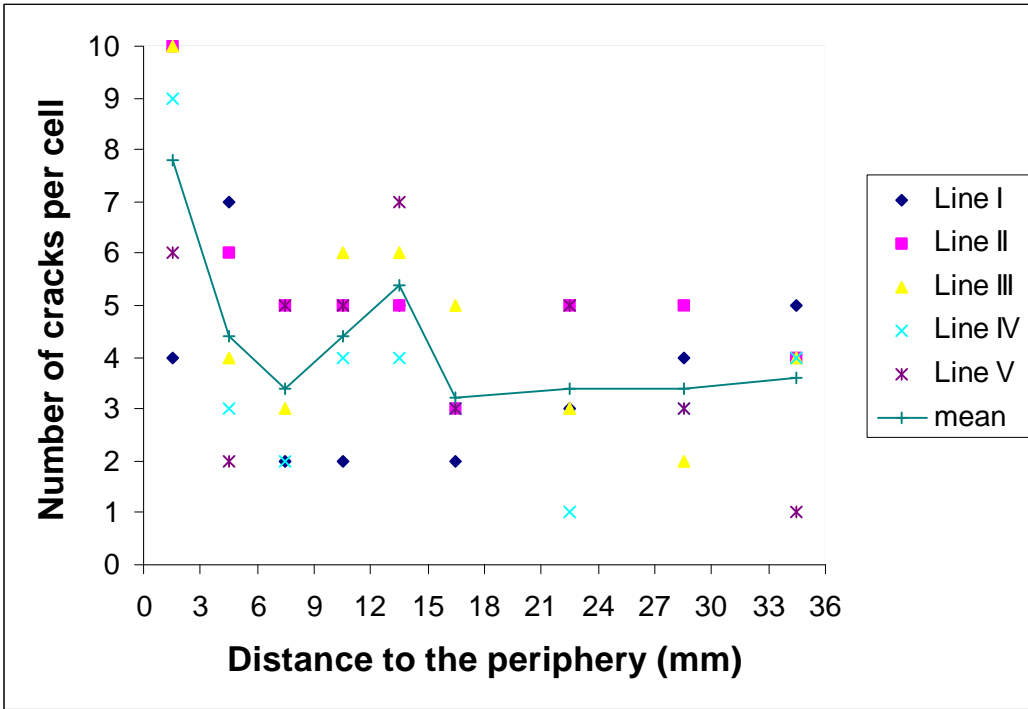


Figure 4.1 KA3065A03 - Number of cracks per cell in sample A1 versus the distance of the cell to the cylindrical periphery of the core.

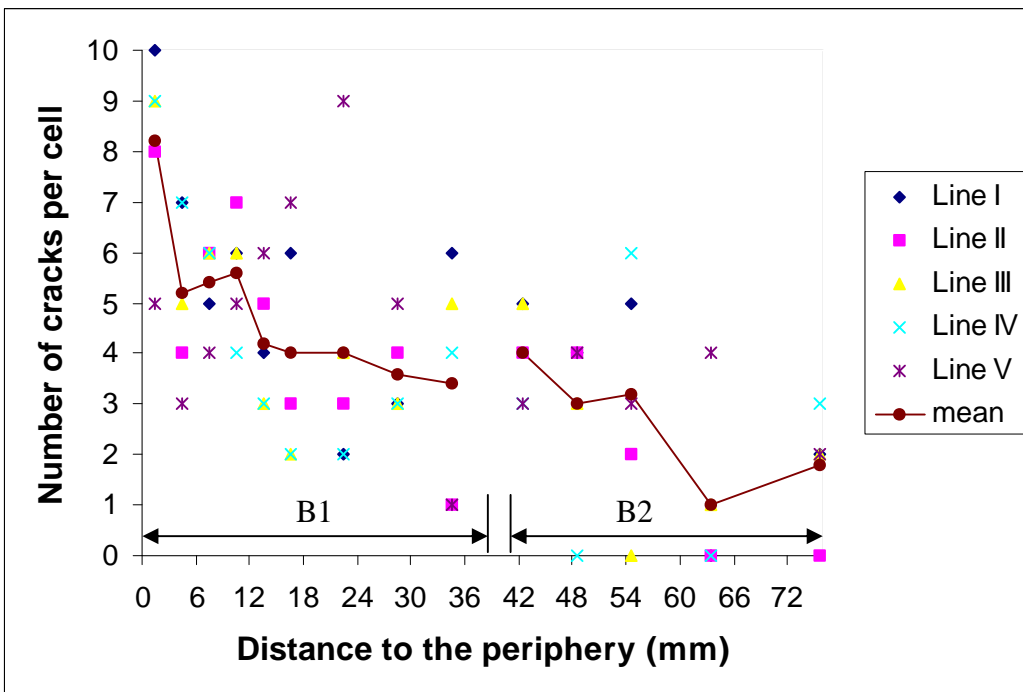


Figure 4.2 KA3065A03 - Number of cracks per cell in samples B1 and B2 versus the distance of the cell to the cylindrical periphery of the core.

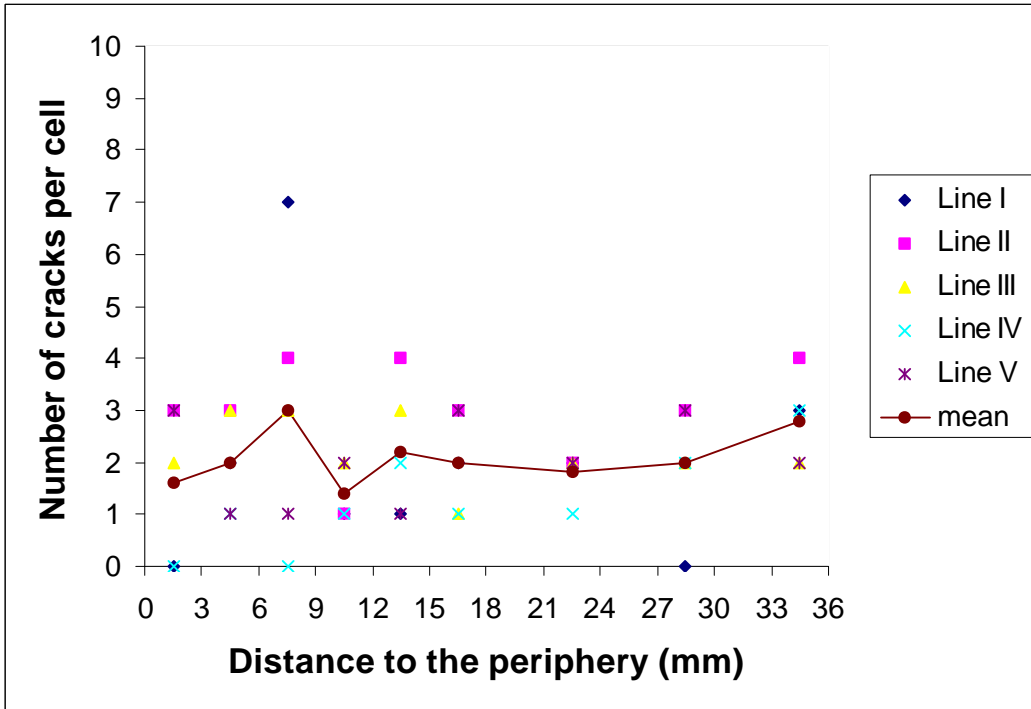


Figure 4.3 KA3065A03 - Number of cracks per cell in sample Ax versus the distance of the cell to the cylindrical periphery of the core.

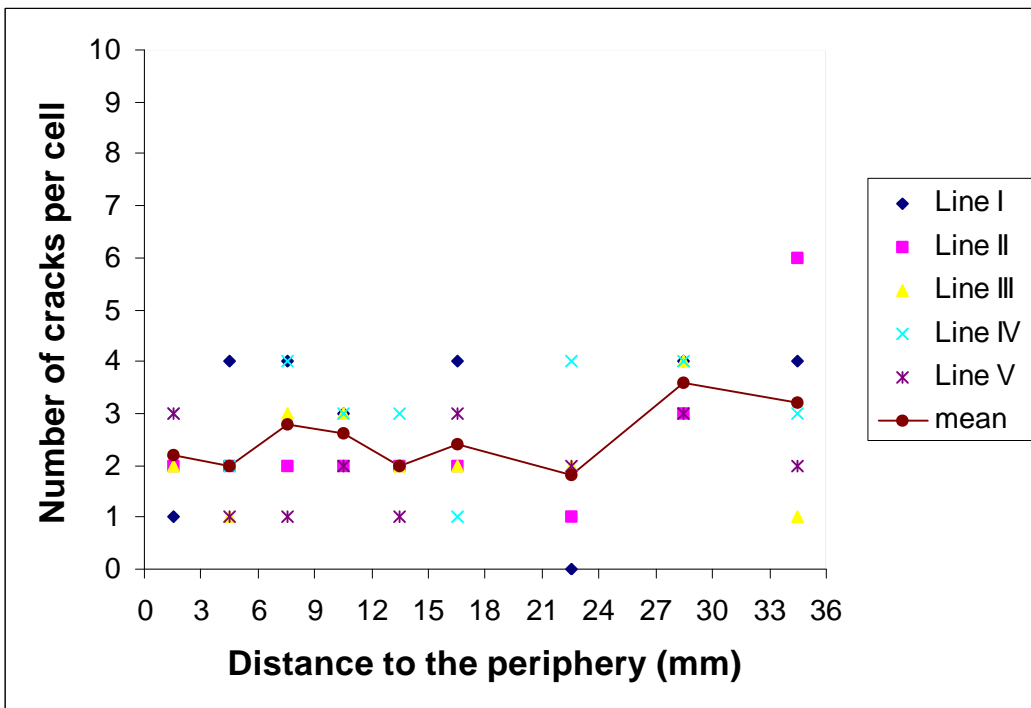


Figure 4.4 KA3065A03 - Number of cracks per cell in sample Bx versus the distance of the cell to the cylindrical periphery of the core.

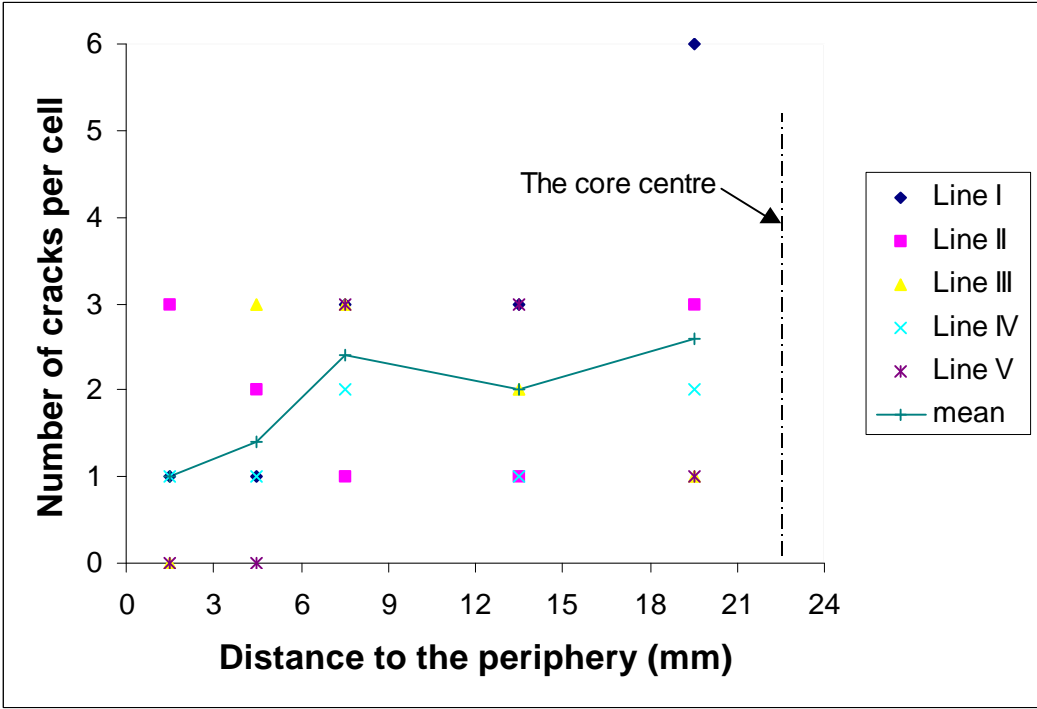


Figure 4.5 KA3065A02 - Number of cracks per cell in sample C1 versus the distance of the cell to the cylindrical periphery of the core.

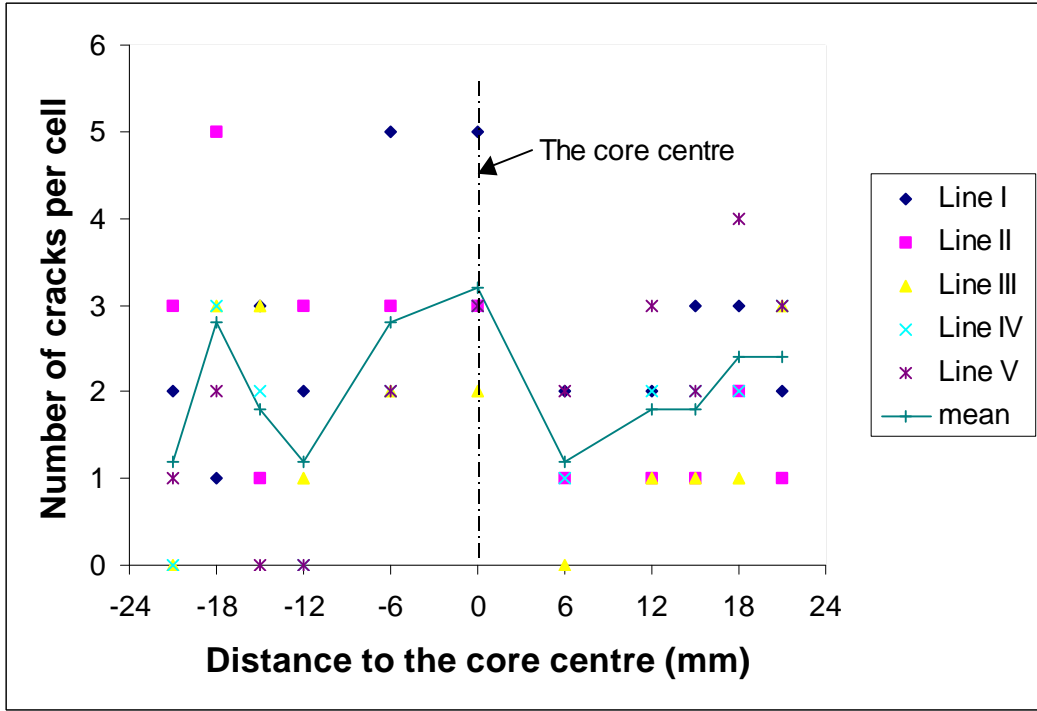


Figure 4.6 KA3065A02 - Number of cracks per cell in the circular sample Cx versus the distance of the cell to the centre of the core.

4.2 Sketches of cracks

In order to demonstrate the pattern of cracks in the thin sections, cracks were sketched in a few cells in samples B1 and Bx. The results of the sketches in the cells 1, 3, 6 and 9 along scan line IV in sample B1 are shown in Figure 4.7. Figure 4.8 illustrates the cracks in the area adjacent to the cylindrical surface of the core, sketched in sample B1. Figure 4.9 shows the cracks in two cells close to the cylindrical surface of the core, one on scan line II and another on IV, in the axial sample Bx.

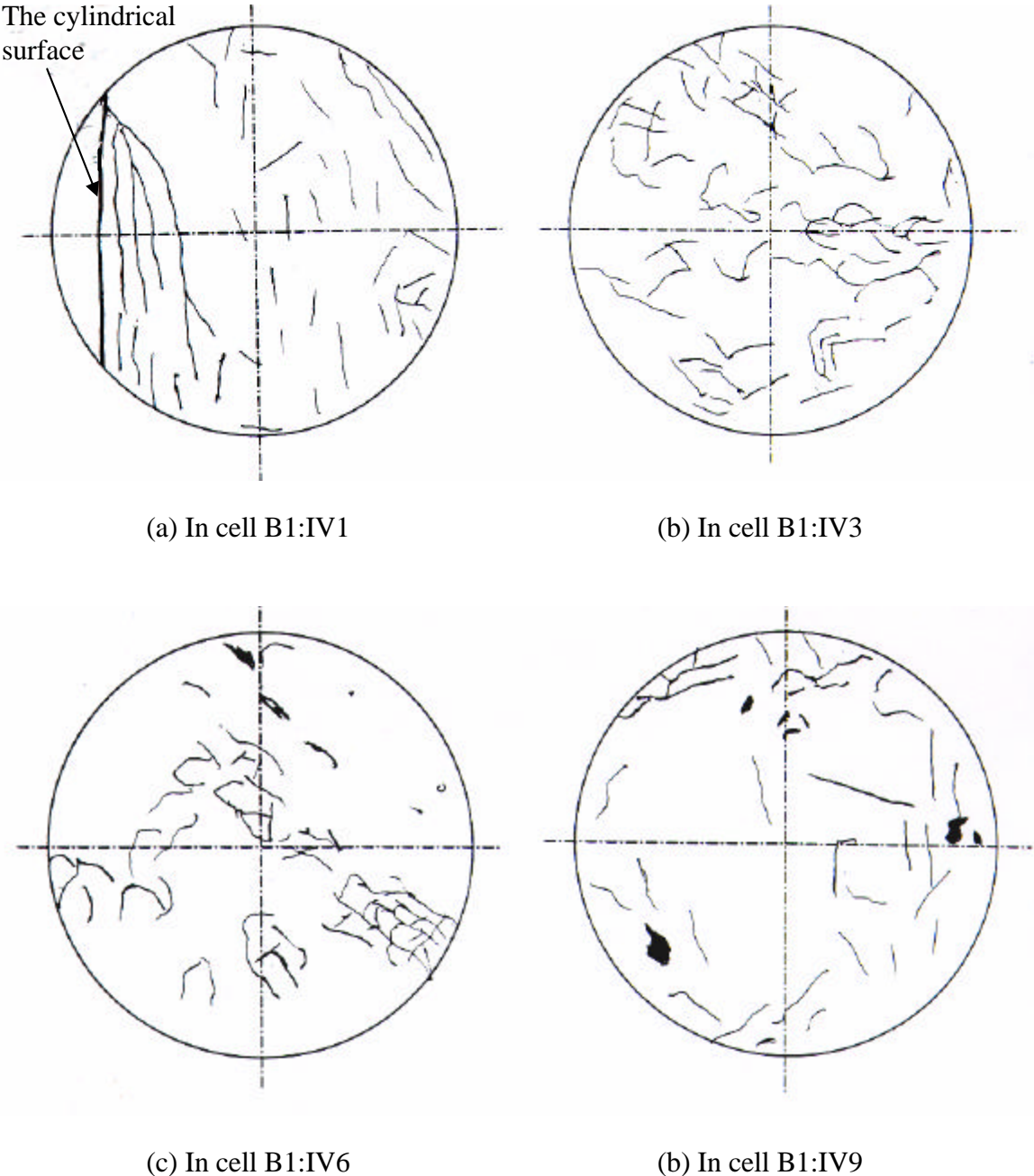


Figure 4.7 KA3065A03 - Sketches of the cracks at four locations along scan line IV in the orthogonal sample B1. The diameter of the cells is 3 mm.

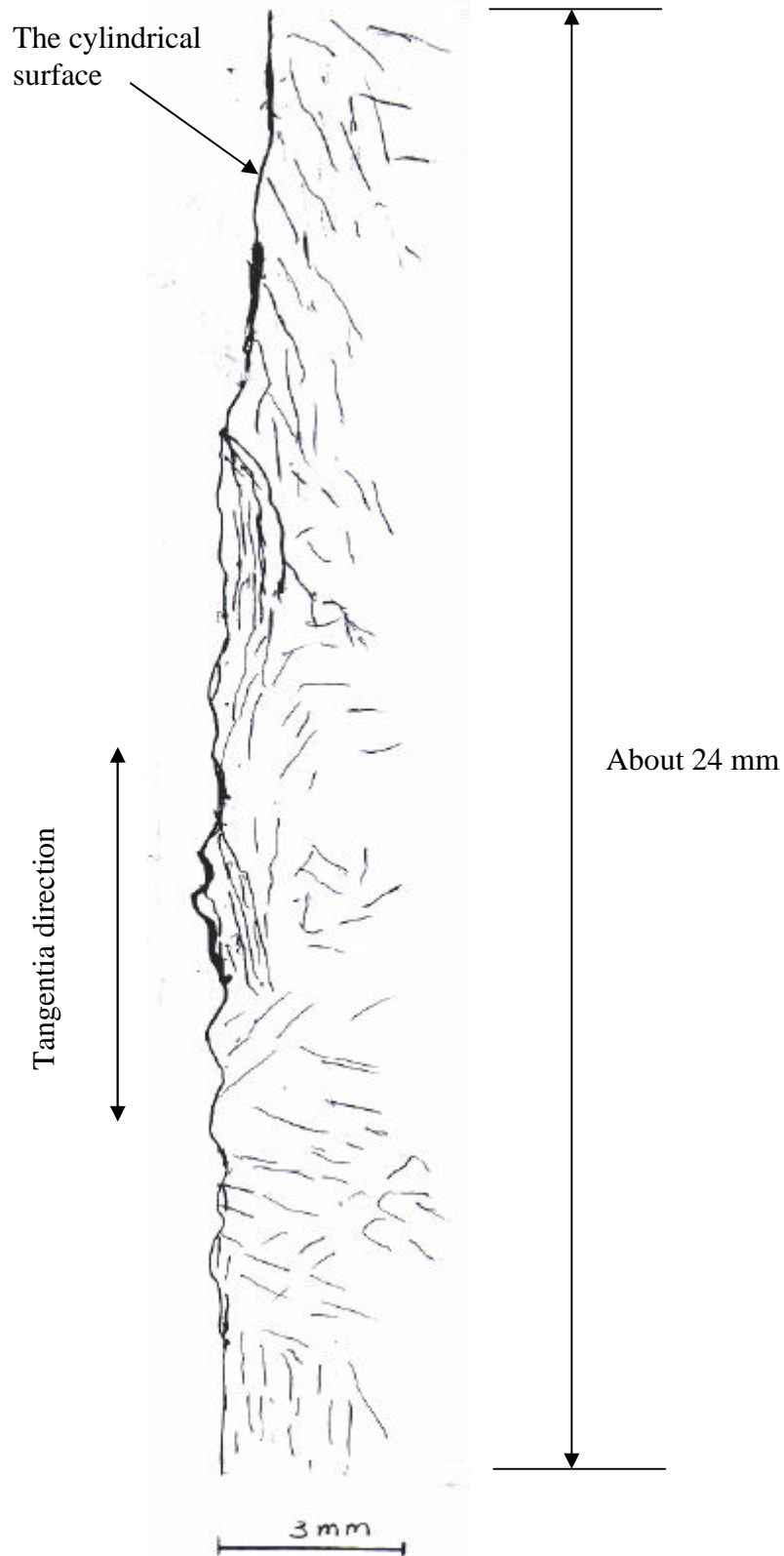


Figure 4.8 KA3065A03 –The cracks in the area adjacent to the cylindrical surface of the core, sketched in the orthogonal sample B1.

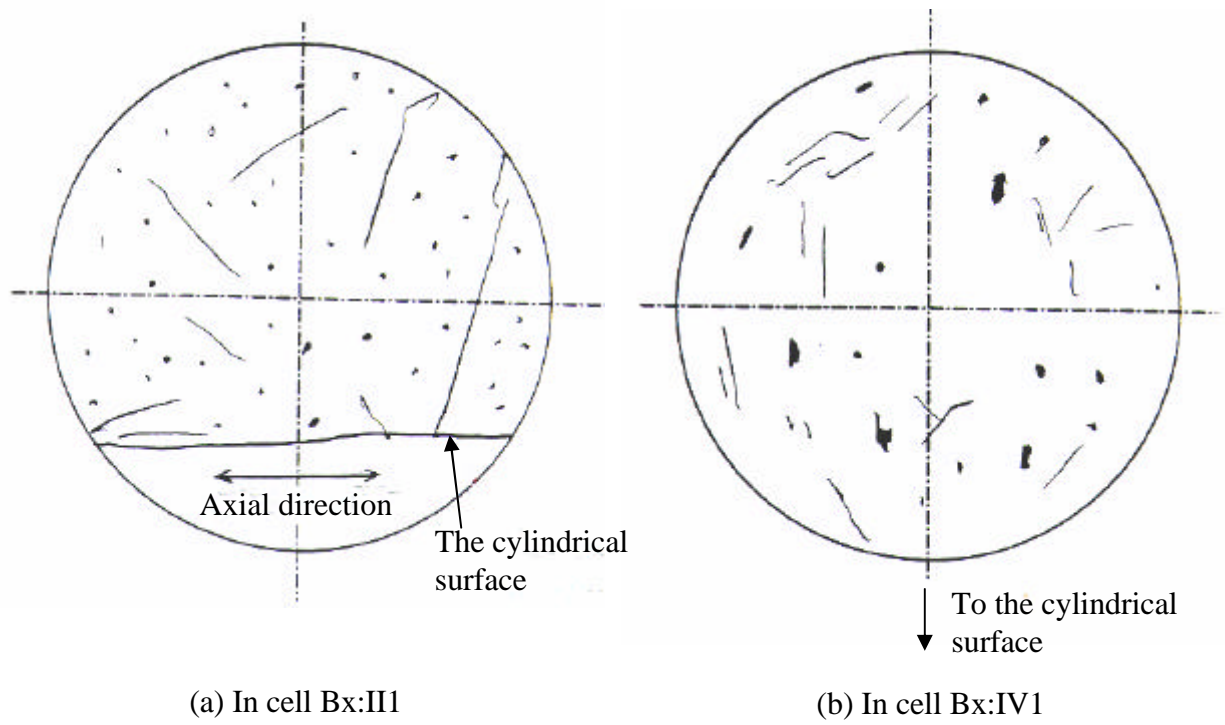


Figure 4.9 KA3065A03 - Sketch of the cracks in the axial sample Bx. Notice that all the cracks and spots in (a) are located in one mineral grain. The diameter of the cells is 3 mm.

5 Discussion

5.1 Distribution of cracks

Samples A1, B1 and B2 were prepared in the cross section of the $\phi 177$ mm core. For these orthogonal samples, it can be clearly seen in Figures 4.1 and 4.2 that a large number of cracks appear in the 3 mm wide area adjacent to the periphery of the core. Beyond the distance of 3 mm, the number of cracks becomes obviously smaller. The average number of cracks per cell in A1 is about 8 in the first 3 mm distance to the periphery and then falls to a level between 3 and 4 beyond the distance of 3mm. In B1 and B2, the average number of cracks per cell is also about 8 in the first 3 mm distance, then falls to a level about 5 in the range from 9 to 12 mm, to a level between 3 and 4 in the range from 12 to 54 mm, and even drops further to a level lower than 3 beyond the distance of 54 mm. It seems that 3 – 4 cracks per cell is the crack density in most of the area of the cross section.

Samples Ax and Bx were prepared parallel with the core axis of the $\phi 177$ mm core. In these two samples, the crack density varies between 2 and 3 cracks per cell. Based on the figures, it is hard to say that the samples have been more seriously disturbed in particular cells.

Sample C1 was prepared perpendicularly to the core axis of the $\phi 45$ mm core. In this sample, the average crack density increases from about 1 crack per cell at the periphery to a level about 3 at the core centre. Sample Cx was prepared parallel with the core axis of the $\phi 45$ mm core. In this sample, the average crack density fluctuates between 1 and 3 cracks per cell along the diameter. An interesting observation is that, as in sample C1, the average crack density in Cx also has its largest value in the centre. It seems that the $\phi 45$ mm core is most disturbed in the centre.

5.2 Heterogeneity in crack distribution

Standard deviation is a proper measure for the variation of a given variable. Here let us define the crack density as the number of cracks per cell and assume that the crack density obeys a normal distribution with respect to the mean value. The distribution of the crack density will look like that shown in Figure 5.1. When standard deviation $\sigma = 0$, it will be a uniform distribution, that is, the cracks are uniformly distributed in the sample, i.e. a homogeneous crack distribution. When σ is small, the crack densities in many places are very close to the mean value. This indicates the sample has a little heterogeneity in crack distribution. However, when σ is very large, the crack densities in many places deviate far from the mean value. This indicates the sample has a great heterogeneity in crack distribution. It is seen in Table 4.1 that the overall standard deviation in the thin sections varies in the range from 0.9 to 2.1 cracks /cell. It can be said that the crack distribution has a certain degree of heterogeneity.

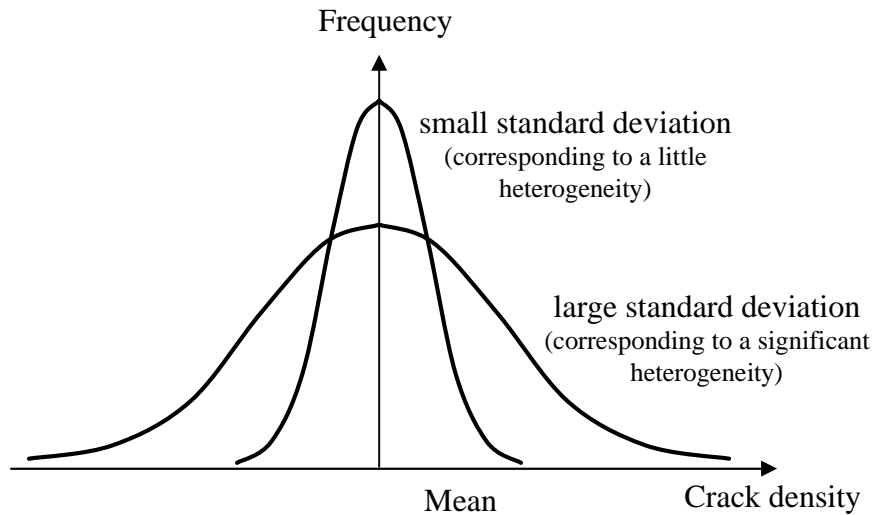


Figure 5.1 Sketches showing two normal distributions.

5.3 Characteristics of cracks

Thin sections from the f177mm core

It is seen in the orthogonal thin sections that cracks are wide and long in a 3mm wide area adjacent to the periphery. The cracks extend straight forward and simply traverse the mineral grains they meet. The cracks in the area close to the periphery are either oriented parallel with the cylindrical surface of the core or are inclined in certain angles to the surface, see Figure 4.7a and Figure 4.8.

With increased distance to the periphery, the cracks becomes thinner and are curled. Furthermore, the pattern of the cracks becomes like a "spiders web" in some places, as shown in Figures 4.7b and 4.7c. It is seen in the microscope that most of these thin and curled cracks are located on the boundaries of mineral grains.

In the thin sections parallel with the core axis, i.e. in Ax and Bx, less number of cracks are observed than in the thin sections perpendicular to the core axis. The significant difference is that a large number of fluorescent "spots" exist in the thin sections parallel with the core axis, see Figure 4.9.

Thin sections from the f45mm core

Not many tangential cracks were observed in these samples. Instead, a small number of wide cracks are distributed all over the cross section of the core. The statistics actually show a tendency that the crack density increases towards the centre of the core, see Figures 4.5 and 4.6.

5.4 Hypothesis for the mechanism of the microcracks

An increase in rock stresses, so-called stress concentration, is created in the rock ahead of the circular slot cut by the drill bit. The stress increase may be so high that tangential and/or inclined cracks are created in the stress concentration area. When the bit proceeds the core is stress relaxed and the tangential cracks are left permanently in the core. These tangential cracks should only be located in a narrow area close to the cylindrical surface of the core if the size of the cut slot is very small with respect to the diameter of the core. The cracks created in this way could traverse mineral grains and would look straight and thick. In the area far from the cut slot, the effect of the stress concentration disappears so that the number of stress-induced cracks would become less with an increase in the distance from the cut slot. When the drill bit proceeds the core is gradually stress relaxed. In a condition of stress relaxation, the mineral grains will elastically expand. The amount of the elastic expansion is different in different mineral grains. This discrepancy in deformation response will result in separation of the grains, i.e. cracks, at their boundaries. This stress-relaxation induced cracks should mainly extend along the grain boundaries so that their pattern looks like a "spiders web". The observed crack pattern in the $\phi 177$ mm core from borehole KA3065A03 may belong to this category.

If the diameter of the core is small, the stress concentration may significantly affect the whole area crossing the diameter of the core. Other crack patterns rather than those in large diameter cores would be created in the entire cross section of the core. The observed crack pattern in the $\phi 45$ mm core from borehole KA3065A02 may belong to this category.

Hakala (1999) conducted a numerical study on the stress distribution in drill cores. The solid core in his model has a diameter of 42 mm. His numerical modelling demonstrated that tensile stresses may occur in three locations in the core: near the drill bit, at the core centre line or on the top of the core. A higher crack density in the interior of the $\phi 45$ mm sample (see Figures 4.5 and 4.6) may be attributed to the tensile stress at the core centre line. The tensile stress at the centre line might disappear if the diameter of the core were large enough. Whether tensile stress occurs at the core centre line in the $\phi 177$ mm core needs to be verified.

It has been found that rock failure in underground structures, such as spalling in mine drift walls, is of tensile even though tensile stress does not exist in the rock mass (e.g. Fairhurst and Cook, 1966). Thus, Stacey (1981) proposed an extension strain criterion for this type of failure. The criterion claims that "fracture of brittle rock will initiate when the total extension strain in the rock exceeds a critical value". It means that extensive cracks may be created in a rock subjected to compression as long as one of the principal strains becomes extensive and beyond a critical limit. Attention should be paid to the extension strain criterion in the future study of core damage.

The measurements conducted by Li (2000) showed that the P wave velocity across the core diameter is 5550 m/s in the $\phi 45$ mm core from borehole KA3065A02, while it is 5780 m/s in the $\phi 177$ mm core from borehole KA3065A03, which is close to the P wave velocity of the undamaged host rock, 5900 m/s, (Pettitt et al., 2000). The P wave velocity measurement shows that the $\phi 45$ mm core has been more damaged than the $\phi 177$ mm core. The wide cracks are concentrated in a narrow area close to the cylindrical surface of the $\phi 177$ mm core, but in the $\phi 45$ mm core the cracks are relatively wide in the entire cross section. This may give an explanation why the P wave velocity is lower in the $\phi 45$ mm core than in the $\phi 177$ mm core even though the average crack density in the $\phi 45$ mm core is smaller.

6 Conclusions

The following conclusions are made on the basis of the microscopic observations of a very limited number of thin sections. The following findings and claims should be verified with more observations in the future.

For the samples from the $\phi 177$ mm core from borehole KA3065A03:

- It is observed in the thin sections orthogonal to the core axis that the crack density in the area close to the cylindrical periphery of the core varies between 5 and 10 cracks per mapping cell (the cell is 3mm wide). In the interior of the core, however, the crack density drops to a level between 3 and 5 cracks per cell and even to a level of lower than 3 if it is far, for instance beyond 54 mm, from the periphery.
- In the thin sections orthogonal to the core axis, cracks are wide, long and straight in the area close to the periphery. The cracks simply traverse the mineral grains that they meet. In the interior, cracks are thin and curled, usually extending along the grain boundaries. The wide and straight cracks close to the periphery may be created due to stress concentration proceeding the advancing drill bit, while the thin and curled cracks in the inside of the core may be due to stress relaxation after coring.
- In the thin sections parallel with the core axis, the crack density remains at a level about 2-3 cracks per cell within the distance from 0 to 36 mm from the cylindrical surface of the core. The crack density in these samples has not an increase in the area adjacent to the periphery as in the orthogonal samples, and the number of observed cracks is less than that in the orthogonal samples. In the axial samples a great number of fluoresced "spots" were observed.
- The fact that the crack density is higher in the orthogonal samples than in the axial samples implies that cracks are preferentially extended in the radial direction of the core.

For the samples from the $\phi 45$ mm core from borehole KA3065A02:

- The average crack density increases from about 1 crack per cell at the periphery to a level about 3 at the core centre in both the orthogonal and the axial samples. It seems that the inside of the core is more cracked than the peripheral area.
- Overall standard deviation of the crack density falls in the range from 0.9 to 2.1 for all the samples, indicating that the samples have a certain degree of heterogeneity in crack distribution.

7 Recommendations

In order to more precisely specify the crack pattern of the cores, the following work is recommended to be carried out:

- Classification of the cracks with respect to their width, straightness, etc.
- Use the cross section of the core for crack mapping.
- Map more thin sections along the periphery of the core to assemble a picture on how the cracks are oriented in the area close to the periphery.

8 Acknowledgement

Andreas Eitzenberger conducted a part of the microscope work.

9 References

Fairhurst, C. and Cook, N.G.W., 1966. The phenomenon of rock splitting parallel to the direction of maximum compression in the neighbourhood of a surface. First Congress of the International Society of Rock Mechanics, Lisbon, Sept. 25-Oct. 1, 1966, Vol.1, 687-692.

Hakala, M., 1999. Numerical study on core damage and interpretation of in situ state of stress. Posiva Technical Report 99-25. ISBN 951-652-080-4/ISSN 1239-3096.

Li, C., 2000. Long term diffusion experiment – Wave velocity measurement on rock cores. Swedish Nuclear Fuel and Waste Management Company, SKB Äspö Hard Rock Laboratory, International Technical Document ITD-00-13.

Pettitt, W., Baker, C. and Young, R.P., 2000. Acoustic emission and ultrasonic monitoring during the excavation of deposition holes in the Prototype Repository. Swedish Nuclear Fuel and Waste Management Company, SKB Äspö Hard Rock Laboratory, International Progress Report IPR-01-01 (in press).

Stacey, T.R., 1981. A simple extension strain criterion for fracture of brittle rock. Int. J. Rock Mech. Sci. & Geomech. Abstr. Vol.18, 469-474.

Appendix – Results of crack count in thin sections

Table A.1 KA3065A03 - Number of cracks per mapping cell in thin section A1.

Cell No.	Distance to "U" edge (mm)	Line I	Line II	Line III	Line IV	Line V	Mean	STD dev
1	1,5	4	10	10	9	6	7,8	2,7
2	4,5	7	6	4	3	2	4,4	2,1
3	7,5	2	5	3	2	5	3,4	1,5
4	10,5	2	5	6	4	5	4,4	1,5
5	13,5	5	5	6	4	7	5,4	1,1
6	16,5	2	3	5	3	3	3,2	1,1
7	22,5	3	5	3	1	5	3,4	1,7
8	28,5	4	5	2	3	3	3,4	1,1
9	34,5	5	4	4	4	1	3,6	1,5
Overall STD dev:								1,3

Table A.2 KA3065A03 - Number of cracks per mapping cell in thin section Ax.

Cell No.	Distance to "U" edge (mm)	Line I	Line II	Line III	Line IV	Line V	Mean	STD dev
1	1,5	0	3	2	0	3	1,6	1,5
2	4,5	2	3	3	1	1	2	1,0
3	7,5	7	4	3	0	1	3	2,7
4	10,5	1	1	2	1	2	1,4	0,5
5	13,5	1	4	3	2	1	2,2	1,3
6	16,5	2	3	1	1	3	2	1,0
7	22,5	2	2	2	1	2	1,8	0,4
8	28,5	0	3	2	2	3	2	1,2
9	34,5	3	4	2	3	2	2,8	0,8
Overall STD dev:								1,0

Table A.3 KA3065A03 - Number of cracks per mapping cell in thin section B1.

Cell No.	Distance to "U" edge (mm)	Line I	Line II	Line III	Line IV	Line V	Mean	STD dev
1	1,5	10	8	9	9	5	8,2	1,9
2	4,5	7	4	5	7	3	5,2	1,8
3	7,5	5	6	6	6	4	5,4	0,9
4	10,5	6	7	6	4	5	5,6	1,1
5	13,5	4	5	3	3	6	4,2	1,3
6	16,5	6	3	2	2	7	4	2,3
7	22,5	2	3	4	2	9	4	2,9
8	28,5	3	4	3	3	5	3,6	0,9
9								
Overall STD dev:								

Table A.4 KA3065A03 - Number of cracks per mapping cell in thin section B2.

Cell No.	Distance to "U" edge (mm)	Line I	Line II	Line III	Line IV	Line V	Mean	STD dev
1	1,5	5	4	5	3	3	4	1,0
2	7,5	4	4	3	0	4	3	1,7
3	13,5	5	2	0	6	3	3,2	2,4
4	22,5	0	0	1	0	4	1	1,7
5	34,5	2	0	2	3	2	1,8	1,1
Overall STD dev:								1,7

Table A.5 KA3065A03 - Number of cracks per mapping cell in thin section Bx.

Cell No.	Distance to "U" edge (mm)	Line I	Line II	Line III	Line IV	Line V	Mean	STD dev
1	1,5	1	2	2	3	3	2,2	0,8
2	4,5	4	2	1	2	1	2	1,2
3	7,5	4	2	3	4	1	2,8	1,3
4	10,5	3	2	3	3	2	2,6	0,5
5	13,5	2	2	2	3	1	2	0,7
6	16,5	4	2	2	1	3	2,4	1,1
7	22,5	0	1	2	4	2	1,8	1,5
8	28,5	4	3	4	4	3	3,6	0,5
9	34,5	4	6	1	3	2	3,2	1,9
Overall STD dev:								1,3

Table A.6 KA3065A02 - Number of cracks per mapping cell in thin section C1.

Cell No.	Distance to "U" edge (mm)	Line I	Line II	Line III	Line IV	Line V	Mean	STD dev
1	1,5	1	3	0	1	0	1	1,2
2	4,5	1	2	3	1	0	1,4	1,1
3	7,5	3	1	3	2	3	2,4	0,9
4	13,5	3	1	2	1	3	2	1,0
5	19,5	6	3	1	2	1	2,6	2,1
Overall STD dev:								0,9

Table A.7 KA3065A02 - Number of cracks per mapping cell in thin section Cx.

Cell No.	Distance to center (mm)	Line I	Line II	Line III	Line IV	Line V	Mean	STD dev
1	-21	2	3	0	0	1	1,2	1,3
2	-18	1	5	3	3	2	2,8	1,5
3	-15	3	1	3	2	0	1,8	1,3
4	-12	2	3	1	0	0	1,2	1,3
5	-6	5	3	2	2	2	2,8	1,3
6	0	5	3	2	3	3	3,2	1,1
7	6	2	1	0	1	2	1,2	0,8
8	12	2	1	1	2	3	1,8	0,8
9	15	3	1	1	2	2	1,8	0,8
10	18	3	2	1	2	4	2,4	1,1
11	21	2	1	3	3	3	2,4	0,9
Overall STD dev:								1,3